

# Ice Shapes on a Tail Rotor

Richard E. Kreeger\*

NASA Glenn Research Center, Cleveland, OH, 44135

Jen-Ching Tsao†

Ohio Aerospace Institute, Cleveland, OH, 44135

**Testing of a thermally-protected helicopter rotor in the Icing Research Tunnel (IRT) was completed. Data included inter-cycle and cold blade ice shapes. Accreted ice shapes were thoroughly documented, including tracing, scanning and photographing. This was the first time this scanning capability was used outside of NASA. This type of data has never been obtained for a rotorcraft before. This data will now be used to validate the latest generation of icing analysis tools.**

## Nomenclature

<i>IGES</i>	=	Initial Graphics Exchange Specification
<i>kts</i>	=	knots
<i>LWC</i>	=	liquid water content
<i>MB</i>	=	megabyte
<i>MVD</i>	=	median volumetric diameter, in microns
<i>psi</i>	=	pounds per square inch
<i>RPM</i>	=	blade rotation speed, rotations per minute
<i>SLD</i>	=	super-cooled large droplet
<i>stl</i>	=	stereolithography format
<i>Ts</i>	=	static temperature
$t_{\text{spray}}$	=	spray time
$V_{\text{tunnel}}$	=	tunnel speed

## I. Introduction

Currently, rotorcraft all-weather operations certification requires substantial data collection through several seasons of flight campaigns or full-scale icing tunnel tests. This is done late in the design cycle and is expensive and time consuming. To address this issue, the community seeks to develop and validate ice accretion simulation tools that are coupled with rotary wing aerodynamic analyses. At the National Aeronautics and Space Administration (NASA), a series of NASA Research Announcement (NRA) investments<sup>1-7</sup> for rotorcraft icing simulation tool development were recently completed. These tools will be useful for the design and certification of rotorcraft for operation in an icing environment.

In order to validate these tools, it is necessary to obtain quality experimental data of ice accretion and shedding under various icing conditions. Full scale icing testing and a flight testing campaign would have been problematic, so NASA, through its partnership with the National Rotorcraft Technology Center (NRTC) and the Vertical Lift Consortium (VLC) collaborated to test a rotor model in the NASA Glenn Icing Research Tunnel (IRT).

Current methods to measure ice accretion shapes are either destructive or primarily two-dimensional, leaving room for improvement with non-destructive, three-dimensional capability. Mold-based methods are capable of capturing the relevant 3D features of an ice shape but require special model considerations such as removable leading edges or parts. They also require moving and handling of the ice shape. There is a cost for materials, and the time required to make a mold can have a significant impact on a test schedule. On the other hand, template-based tracing methods, while much quicker and cheaper, can only capture the ice shape along a fairly limited number of two-dimensional cuts.

\* Aerospace Engineer, Icing Branch, 21000 Brookpark Rd., MS 11-2, AIAA Associate Fellow.

† Principal Research Scientist, Ohio Aerospace Institute, Associate Fellow AIAA.

There are three uses for digitized ice shapes: (i) data analysis and archiving, (ii) production of models for aerodynamic testing and (iii) development of meshes for computational fluid dynamics. The data analysis and archiving task must be accomplished first, and the application to the helicopter problem introduced a number of unique challenges.

In order to obtain the ice accretion data for tool validation, it was necessary to develop a robust and affordable means of recording and archiving fully three-dimensional (3D) descriptions of experimental ice accretion geometry. The approach chosen to do this was to apply a commercial laser scanning system that has been validated for use in the icing tunnel.<sup>8</sup>

NASA has tried to scan ice shapes before, but what makes it possible now is the advancement of the state-of-the-art in commercial laser scanning.<sup>9,10</sup> In particular, it is the accurate, portable and reliable Romer arm and scanner combination (able to operate at IRT temperatures) and the robust algorithms of the Geomagic software. The Romer Absolute system was identified as the scanner and arm most suitable for use in the IRT for this test.

Applications which push the state-of-the-art require 3D data: (i) swept wings, (ii) rotor blades and (iii) in the future perhaps engine components. A number of IRT tests have already been conducted to develop 3D scanning capabilities for ice shapes on fixed wings. A variety of ice shapes and airfoils have been successfully scanned to determine the limits of the capability, including roughness, runback ridge, streamwise rime, double-horn glaze, developing scallops and full scallops. Only the full scallop shape and very fine rime roughness provided significant challenge to the hardware and software. The scanner was able to digitize initial roughness shapes which could not be captured at all by simple 2D techniques, such as hand tracing. Thus, NASA was able to demonstrate the system and procedures using fixed airfoils and was ready to apply it to a rotorcraft application.

## II. Background

A three-week test in the Icing Research Tunnel was conducted to generate data that will be used to validate the latest generation of icing analysis tools for rotorcraft. The Vertical Lift Consortium (VLC) provided the model, along with the personnel to operate it, and this was the first rotating model in the IRT in twenty years.

The test had multiple objectives, including ice accretion, ice shedding trajectory and impact, deice and anti-ice system performance, and rotor performance. High quality data for rotor blade icing was obtained. Data included rotor ice shapes, rotor performance, deice and anti-ice performance with runback/refreeze, shed ice trajectories and impact data. Ice shapes were documented by 3D laser scan, hand tracing and photograph. High speed video was also taken. A total of 89 runs were completed.

The model was based on a Bell 206B tail rotor system in order to represent a scaled down main rotor. This is similar in concept to a model which was previously tested in the IRT<sup>11</sup>.

The model used two production tail rotor blades of stainless steel construction with a stainless steel leading edge, stabilized with a honeycomb core. The blade chord was 5.25 in., and there was no twist. The rotor disc was 65 inches in diameter. The system was designed as a two-bladed teetering rotor that would flap aft with airspeed and thrust.

Heater blankets were installed on the leading edge, incorporating six independent heater zones. These could be cycled simultaneously in any combination to recreate any type of de-icing scheme or turned on continuously to simulate various anti-icing schemes. The heating elements were embedded within the internal surface of the blades. Both internal and external temperature sensors were also installed.

The blade system was installed on a custom built test stand designed to allow for the measurement of rotor loads and utilized a 5-component balance. The rotor was driven by an electric motor through a drive system specifically designed for this model. Likewise, the data acquisition and control systems were custom to this model.

The model was heavily instrumented in both the rotating and non-rotating frames. Key measurements included blade temperature, rotor loads, blade strains, model vibration, motor temperature, drive system temperature and heater blanket electrical power were measured. Although these measurements were taken during testing, they are not presented here.

Several notable firsts for the IRT were accomplished during this test: (1) first ever electro-thermal de-icing of a rotating scale model, (2) first capture of a rotor shed event with a high speed Phantom camera, (3) first ever super-cooled large droplet (SLD) cases on a rotating blade and (4) first use of a 3D scanner to record ice shapes on a rotor blade. The rotor icing test was the first use (in the IRT) of the scanner capability on a model that was not primarily designed for the purposes of selecting, optimizing or validating the scanner hardware or process.

### III. Scanner Procedure

The basic procedure used during this test will be discussed, along with some key lessons learned. A detailed checklist of the best-practice scanner procedures was refined during this IRT test. The complete best-practice method for post-processing will appear in a separate document.

#### A. Pre-Test

Components necessary before the test include (1) scanner and equipment, (2) paint equipment and (3) magnetic base.

For this test, a Romer 7 Axis SI arm with integrated scanner was used, including removable cover, removable lock, power cable, USB cable, network cable and tripod. The laptop PC used to drive the scanner used Geomagic Studio Version 13. The key advantages of this software are operability with the scanner arm and the robustness of the post-processing algorithms. The hardware requirements for the scanner laptop were higher than standard business-laptop, the main requirement being primarily a higher-end graphics card.

It is possible to run the software from the control room. Using this method, it is difficult for the scanner operator to see the screen. This sort of real-time feedback during the scanning process is beneficial for getting more complete coverage. Many prior attempts had been made in which the control laptop was brought into the test section along with the scanner. Temperature issues had never been encountered. Based on these experiences, it was actually more time-efficient to bring the laptop into the test section with the scanner, and for this reason a lightweight portable cart was used.

Paint equipment included a spray gun, either the Binks-type or the airbrush type. A magnetic base, used previously at NASA, was used to maintain scanner location during each scan.

#### B. Preparation

This phase included photographing the ice, locking in the model, masking the model, painting the model, and adjusting tunnel lighting. It is required that the model not move during the scan process. This test used a specially-made jig.

Due to the transparency of ice, painting (a form of powdering) of an iced surface is required. Even the most opaque rime ice is partially transparent to the optical scanner, thus it is necessary to coat the ice using a specially-designed paint. The current formulation is based on a titanium dioxide pigment in a quick evaporating solvent, such that the hand spray deposition method applies only a thin, uniform layer of paint to coat the surface of the ice. The solvent evaporates quickly, leaving only the powder. The procedure requires the use of a pressure regulator to control the shop air into the paint sprayer. Typically, a setting of  $25 \pm 5$  psi works well. Due to the small areas of ice being scanned, an airbrush type sprayer was used exclusively during this test. It was necessary to mask the model to prevent overspray of paint onto the non-metallic areas of the blade. Overspray is fine onto aluminum or stainless steel models. The process of locking the model and painting is shown in Figure 1.

Once the ice was prepared with paint, pre-scan activities included staging the equipment into the tunnel, launching the software and establishing connection. High intensity illumination or other bright lights in the test section are turned off prior to scanning. Some normal lighting is necessary to work in the test section, but high intensity light is not desired because it reduces the contrast between the laser and the painted ice. The Romer specifications call for temperatures between 15 and 35-deg C, but we have successfully conducted numerous scans in the IRT test section with temperatures below this. The tunnel crew typically kept the fan at idle speed (less than 15 knots) during the preparation and scanning procedures, in order to maintain the ice at cold temperature.

#### C. Scan

A typical scan of 12-24" of span and about 6-8" of chord took about 20-25 minutes, and required 2 people. This was roughly comparable to the 10-15 minutes required for getting 3-6 hand tracings, except of course the scanner provides a fully-3D representation. In general, using the scanner took about 10 minutes longer than runs requiring tracings only. The scanning process is shown in Figure 2.

Proper technique involves carefully scanning three regions in two directions- making both horizontal and vertical passes, with vertical passes being chordwise. The three regions are the pressure side, the leading edge and the suction side. For best results, the operator moves the scanner evenly at approximately 1-inch per second, minimizing any back-tracking during a given pass. The arm will alert the operator if any one joint on the arm is overextended beyond the calibrated limits, but data will continue to record. This can cause incorrectly positioned scans if not corrected immediately. When not taking data but still controlled by the scanner, the operator can move the view on the screen. Each scan consists of multiple ordered point cloud objects.

#### **D. Data Reduction**

Post-test cleanup and closing of scans takes anywhere from 20 minutes to 16 hours, depending on the ice shape and on the skill of the operator. Deep scallops are the most challenging and require manual cleanup. Two million points (triangles) turns out to be the practical upper limit for processing on an Intel i7. Typical scan size is 30 million points with a file size of 1.0 to 1.5 GB for the raw data. The procedure also requires a high quality video card, especially for manual cleanup.

Each scan consists of a number of multiple point cloud objects in an ordered format, which must then be processed through a procedure called registration. Multiple scans are aligned to a world-axis system using an optimal point cloud fitting/uniformity between the scan objects. This re-orientes the scan objects that share similar regions and translates them slightly so as to construct a complete object. A setting of 0.004" was used for the maximum allowable translation. Registered and aligned data is then combined into a single point cloud object which can then be converted into a polygon surface using a wrapping process. Once the multiple ordered point clouds are combined into one object, they are automatically converted into an unordered point cloud. Unordered point clouds differ slightly from ordered point clouds, in that they are not connected by quadrilateral regions and have a variable density.

A polygon object or mesh is a construction of triangles that defines the scanned geometry. The user specifies the number of triangles to be used to define the object's geometry, and in most cases two million triangles was used. Increasing the number of triangles increases the time needed to construct the initial mesh and the time needed to make subsequent repairs. Point cloud wrapping involves a number of key parameters over which the user has control, such as noise reduction, inclusion of small or island components, and the maximum number triangles. A polygon wrap may not be water-tight initially and usually requires subsequent modifications (called repairs) which can be significant.

Once the initial surface wrap is completed, the result of which is a polygon object consisting of a number of triangles, the surface can then be further edited using a variety of mesh repair tools. The user can specify a number of parameters to analyze and modify during this clean-up stage. Non-manifold edges are triangles on the natural boundary of the object, but not connected on two of the triangle's sides. Self-intersections are triangles that are tangled or intertwined with neighboring triangles. Highly-creased edges and spikes are usually left intact, since ice geometry often includes highly curved areas. Small components are free standing triangles that are few in number. Small tunnels are double-layered constructs in the mesh having both a front and back opening. Small holes are openings in the polygon mesh small enough to be filled in automatically.

The Geomagic software includes several techniques to fill holes, both large and small. Fill techniques available are curvature, tangent and flat. Tangent fill was used for completing the water-tight surfaces, because curvature rounded the local ice shape in ways that were obviously less natural, while flat fills resulted in plateau-looking structures. Fill modes can be complete, partial or bridge. A complete fill acts on a closed boundary. A partial fill acts between two selected points and a boundary. Bridge fill covers from a selected boundary to another selected boundary. On some of the more complex scans, manual fill of single individual holes was necessary.

Post-processed scans can be saved as stereolithography (stl), IGES, or a variety of other formats. Stereolithography and native Geomagic Wrap files (triangular mesh formats) are the only means to maintain all of the details of the scan. Converting the scan into a CAD format such as STEP or IGES results in a significant loss in detail. Some post-processing can also be done in other environments, such as the Rhino software package.

#### **E. Hand Tracing Procedure**

Two-dimensional tracings were taken at up to six locations along one blade using prefabricated cardboard templates. Trace stations were marked on the external surface of the blades, with the exact locations documented in the test report. Four of the locations were near temperature sensors installed internally and externally on the blade in order to provide temperature data for CFD comparisons. Tracings can have offsets which are not immediately apparent if the template is not fully seated. The software package SigmaScan was used to digitize and post-process the hand tracings.

### **IV. Results**

Eleven ice shapes were obtained during the three-week test entry, as shown in Table 1. The ice shape data are being used to validate the newest generation of rotorcraft ice accretion prediction codes.

#### **A. Clean Blade Analysis**

Prior to installation, the clean blades were scanned. There were two primary and two alternate blades. The two primary blades were production tail rotor blades. A fixture to hold the blade during scanning was instrumental. The two primary blades were designated “red” and “white,” of which only the red article will be discussed here. When scanning a clean blade, it was not necessary to paint the model.

The initial scan was more than 108 million points. It was aligned to the world and wrapped using best practices, including sampling. This got it down to 2 million points. From here I am able to make cuts, export it as an stl file, and compare it to the idealized IGES file using best-fit alignment.

This is useful for the following reasons. No exact CAD model of the blade was available and the CFD surface grid used for this blade was based on an idealized IGES file. With the scan data, the exact blade, which was a one-of-a-kind build-up on an existing blade, can be documented

The scanner was able to pick out very fine features, more so than expected. For example, the scan data clearly recorded the lines drawn on the exterior of the blade, in order to indicate where 2D tracings were to be made. It also picked up slight impressions in the blade surface from the heater wires underneath (visible near the leading edge in the rendered image in Figure 3). These were features not visible to the eye. Other as-built features were also discernable from the scans. For example, the propeller tape used on the installed model during runs (visible near the tip in Figure 4) is another geometric feature which is quite easily measurable by the scanner, as long as the surface is painted. The highly-detailed geometry of the blade tip (see also Figure 4, for example) can then be easily recorded.

## **B. Scanner Settings**

Scanner settings can impact the procedure. One such setting which has never before been addressed is resolution. A higher resolution can capture smaller features, but can potentially make closing the shape more difficult. Higher resolution also makes the file size much larger, due to the number of points, but this is not a practical limitation with a capable computer. There is a small savings in the time it takes to scan that can be realized by using a lower resolution. Determining the difference will allow future tradeoffs between detailed measurements and post-processing time. As an example of these tradeoffs, Figure 4 shows a side-by-side comparison between a photograph of the ice near the tip with a closed scanner shape. Run 53, featured in Figure 4, was scanned twice, once using the normal scanner setting (spacing of 0.001-inches) and again using a lower-resolution setting (spacing of 0.0109-inches). This significantly reduced the size of the raw data file, from 391MB to 17.9MB. One of the features available in the Geomagic software is a comparison feature. When these two scans were closed and then compared, the average deviation between the two scans was +/- 0.0203 inches. This amount of uncertainty can be significant depending on the type of ice feature being resolved. Note that some of the small features have been rounded off as part of the data closure process, but that other small features have been accurately retained. Major features, for example radial location of ice shedding, or horn height, are not affected at all, based on this preliminary study. While this comparison was made for a single run and cannot be considered comprehensive, it at least provides some indication that, even at lower, less-aggressive hardware settings the scanner is capable of picking up the at a minimum, the majordetails of a typical ice shape.

## **C. Comparisons to Ice Tracings**

Typically, hand tracings were only made at six designated radial locations. If there was no or insufficient ice at a station, no tracing was taken.

Typically as part of the ice scanning process, hard probes of known geometric reference points are taken to align the scan data to the model coordinate system. This model had a few unique features which made the standard geometry definition protocol insufficient. First, the model was based on production article blades, hence it could not be equipped with reference probing points. Since the model was free to rotate when powered-down, there was no reasonable way to clock the blades to the same azimuth for scanning, within the accuracy required. For these reasons, the ice shape scans could not be aligned with the clean blade using the preferred methodology. Instead, it was necessary to take detailed scans of the entire blade tip area, and align the ice shapes with the clean blade by aligning these geometric features. This method introduces a very small amount of uncertainty near the tip which may increase towards the root. In Figure 5, a scanned ice shape has been post-processed and then superimposed over the scan of a clean blade.

The advantage of the scanner is that tracings can be taken at any spanwise station. At the stations where 2D hand tracings were obtained, it is possible to make comparisons. Another advantage of the scanner is that it can measure ice that is too small to trace. Comparisons have been made between hand tracing and 2D section cuts. The scanner approach is capable of an accuracy of 0.003” (based on spacing) compared to an estimated 0.05” that can be reasonably obtained with a hand-tracing.

A cold blade run (Run 53) is shown in Figure 6, in which the 2D tracings of the cold blade are plotted along with the ice shape. Four 2D tracings have been digitized and superimposed on a 3D scan at the proper locations. It is possible to determine for each station the nature of glaze, rime, mixed conditions, etc., based on known parameters including radial location and blade r.p.m. as well as the tunnel conditions such as temperature, liquid water content, drop size and tunnel speed. This analysis, when combined with the photographs and the full 3D scan, allows a quantification of the spanwise variability features of 3D ice shapes. It will also allow a much better capability for modeling shed events, and partial shed events.

## V. Conclusion

A robust and affordable means of recording and archiving fully 3D descriptions of experimental ice accretion geometry has been developed for use in the icing tunnel. The system and procedures developed were able to accurately capture the aerodynamically relevant features of ice shapes during the first operational use for a rotorcraft application. The 3D ice accretion measurement capability was achieved for eleven ice shapes, including cold blade, self-shedding, SLD, deicing and anti-icing shapes. This type of data has never been obtained for a rotorcraft before. This data will now be used to validate the latest generation of icing analysis tools.

## Acknowledgments

The authors would like to acknowledge the NRTC/VLC high-fidelity icing team, especially Jason Wright and Roger Aubert (Bell Helicopter Textron), Peter DeVito and John O'Neill (Sikorsky), Bob Narducci, Tonja Reinert and Ed Brouwers (Boeing) and Eliya Wing (Georgia Tech). The authors would also like to thank Mr. Chris Lynch for his excellent imaging work during the experiment. In addition, none of this would have been possible without the dedication and professionalism of the technicians and engineers of the Icing Research Tunnel.

## References

- <sup>1</sup>Narducci, R., and Kreeger, R., "Analysis of a Hovering Rotor in Icing Conditions," presented at the American Helicopter Society 66<sup>th</sup> Annual Forum, Phoenix, AZ, May 11-13, 2010.
- <sup>2</sup>Narducci, R., Orr, S., and Kreeger, R., "Application of a High-Fidelity Analysis Method to a Model-Scale Rotor in Forward Flight," presented at the American Helicopter Society 67<sup>th</sup> Annual Forum, Virginia Beach, VA, May 3-5, 2011.
- <sup>3</sup>Kinzel, M., Sarofeen, C., Noack, R., and Kreeger, R., "A Finite-Volume Approach to Modeling Ice Accretion," AIAA 2010-4230, 28<sup>th</sup> AIAA Applied Aerodynamics Conference, Chicago, IL, 28 June- 1 July, 2010.
- <sup>4</sup>Sarofeen, C., Kinzel, M., Noack, R., and Kreeger, R., "A Numerical Investigation of Droplet/Particle Impingement on a Dynamic Airfoil," AIAA 2010-4229, 28<sup>th</sup> AIAA Applied Aerodynamics Conference, Chicago, IL, 28 June- 1 July, 2010.
- <sup>5</sup>Sarofeen, C., Noack, R., and Kreeger, R., "A Non-Cut Cell Immersed Boundary Method for Use in Icing Simulations," AIAA 2012
- <sup>6</sup>Rajmohan, N., Bain, J., Nucci, M., Sankar, L., Flemming, R., Egolf, A., and Kreeger, R., "Icing Studies for the UH-60A Rotor in Forward Flight," presented at the American Helicopter Society Aeromechanics Specialists Conference, 20-22 January, 2010.
- <sup>7</sup>Nucci, M., Bain, J., Sankar, L., Kreeger, R., Egolf, A., and Flemming, R., "Assessment of the Effects of Computational Parameters on Physics-Based Models of Ice Accretion," AIAA 2010-1277, 48<sup>th</sup> Aerospace Sciences Meeting, 4-7 January, 2010.
- <sup>8</sup>Lee, S., Broeren, A., Addy, H., Sills, R., and Pifer, E., "Development of 3D Ice Accretion Measurement Method," AIAA 2012-2938, 4th AIAA Atmospheric and Space Environments Conference, 25-28 June, 2012.
- <sup>9</sup> Desktop Engineering magazine, July 2013, "Metrology Meets Meteorology."

<sup>10</sup>. Aerospace America magazine, February, 2014, “Laser Eye on Aircraft Ice.”

<sup>11</sup>. Miller, T., and Bond, T., “Icing Research Tunnel Test of a Model Helicopter Rotor,” AHS 45<sup>th</sup> Annual Forum, May 22-24, 1989; Boston, MA

## Tables and Figures

**Table 1 Summary of Run Conditions**

Run Condition	Run Number	Airspeed (knots)	RPM	MVD ( $\mu\text{m}$ )	LWC ( $\text{g}/\text{m}^3$ )	Collective. (deg.)	Static Temp. ( $^{\circ}\text{F}$ )	Spray Time (min.)
Cold blade	29	60	1200	15	0.50	2	14	3:00
Cold blade	47	60	2100	15	0.50	2	14	1:00
Cold blade	53	60	1200	15	0.50	2	14.2	3:00
Cold blade	54	60	2100	15	0.50	8	15	1:00
Self shed	55	150	2100	15	0.50	2	16.9	1:30
Chordwise de-ice	65	60	2100	15	0.50	5	-4	5:18
SLD Cold Blade	68	150	2100	110	0.50	5	-4	1:00
Spanwise de-ice	76	150	2100	15	0.50	5	-4	5:22
SLD Cold Blade	81	150	2100	110	0.50	2	-4	1:00
Self shed	82	60	2100	15	0.50	2	14	2:30
Self shed	83	60	2100	15	0.50	2	9	3:00



**Figure 1. Painting the Ice.**



**Figure 2. Scanning the Ice.**

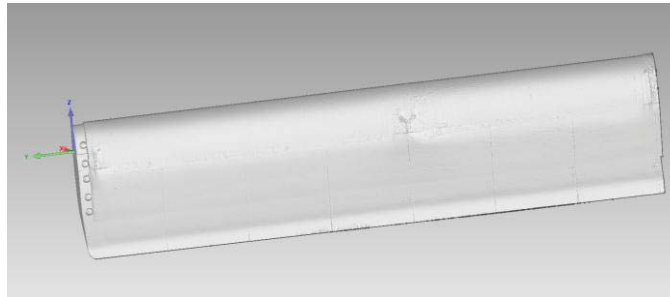


**Figure 3. Clean Blade (Red).**

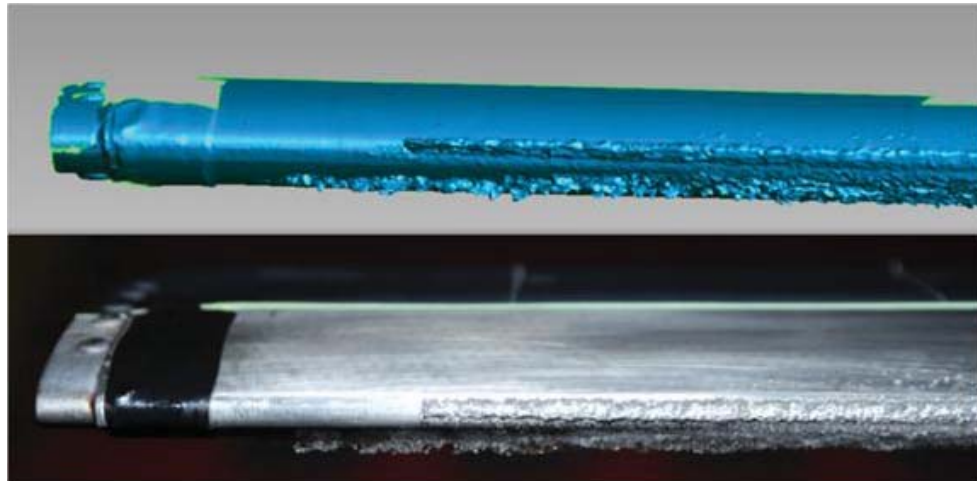


**Figure 4. Comparison of Scan with Photograph (Run 54).**

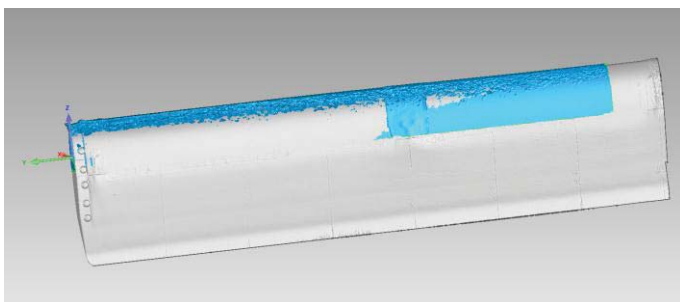


**Figure 5. Scanned Clean Blade with Scanned Ice Shape. (Run 53)**

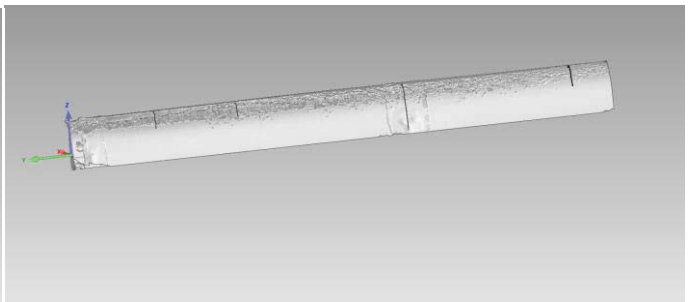


**Figure 6. Scanned Ice Shape with Digitized Tracings. (Run 53)**